Supplementary information

Declining precipitation frequency drives earlier leaf senescence by intensifying drought stress and enhancing drought acclimation

This PDF includes

Figure S1-S8

Table S1-S2

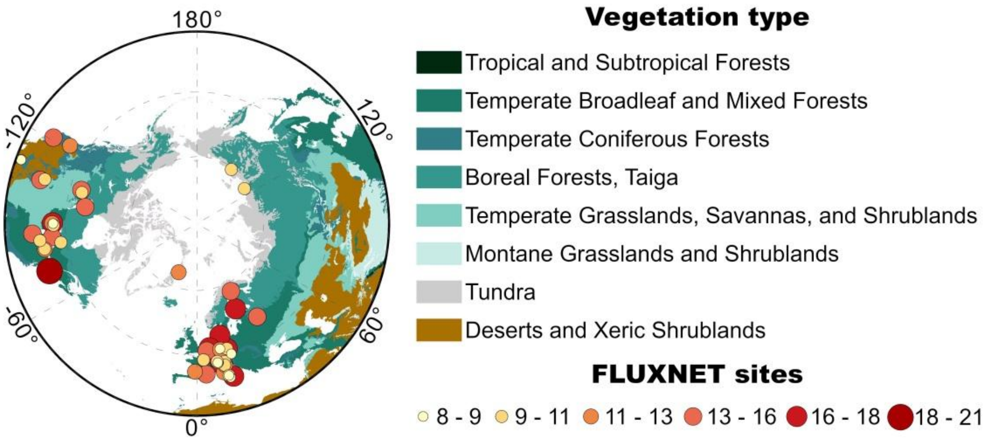

Figure S1 Description of the study area and flux sites used in this study. The number of sites indicated by the size of circles and detailed information of sites are provided in Table S2.

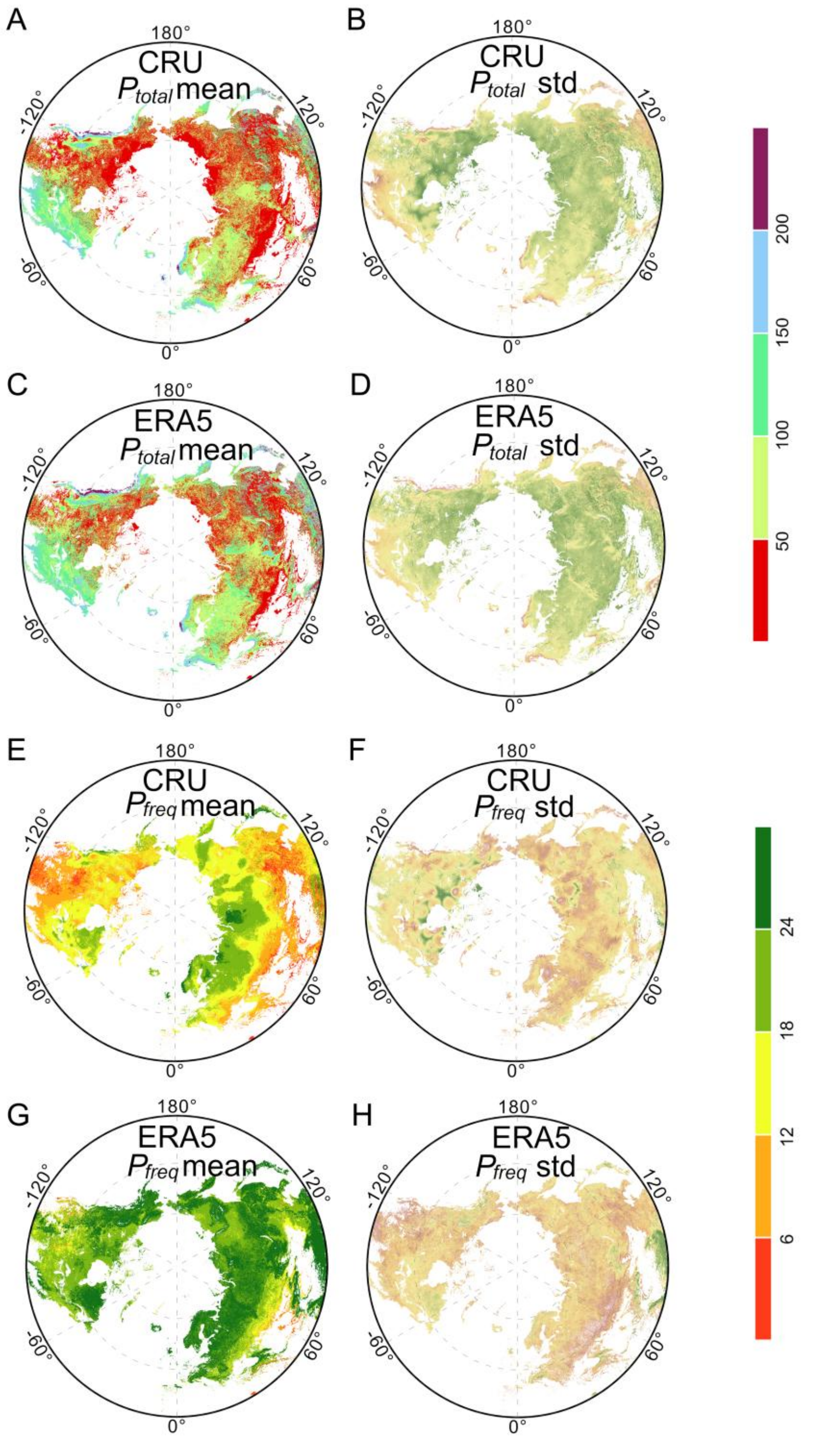

Figure S2 Mean preseason total precipitation (P_{total}) and its standard deviation (Std) for (A-B) CRU and (C-D) ERA5 observations over 1982-2022. E-F represent precipitation frequency (P_{freq}) for these two observations.

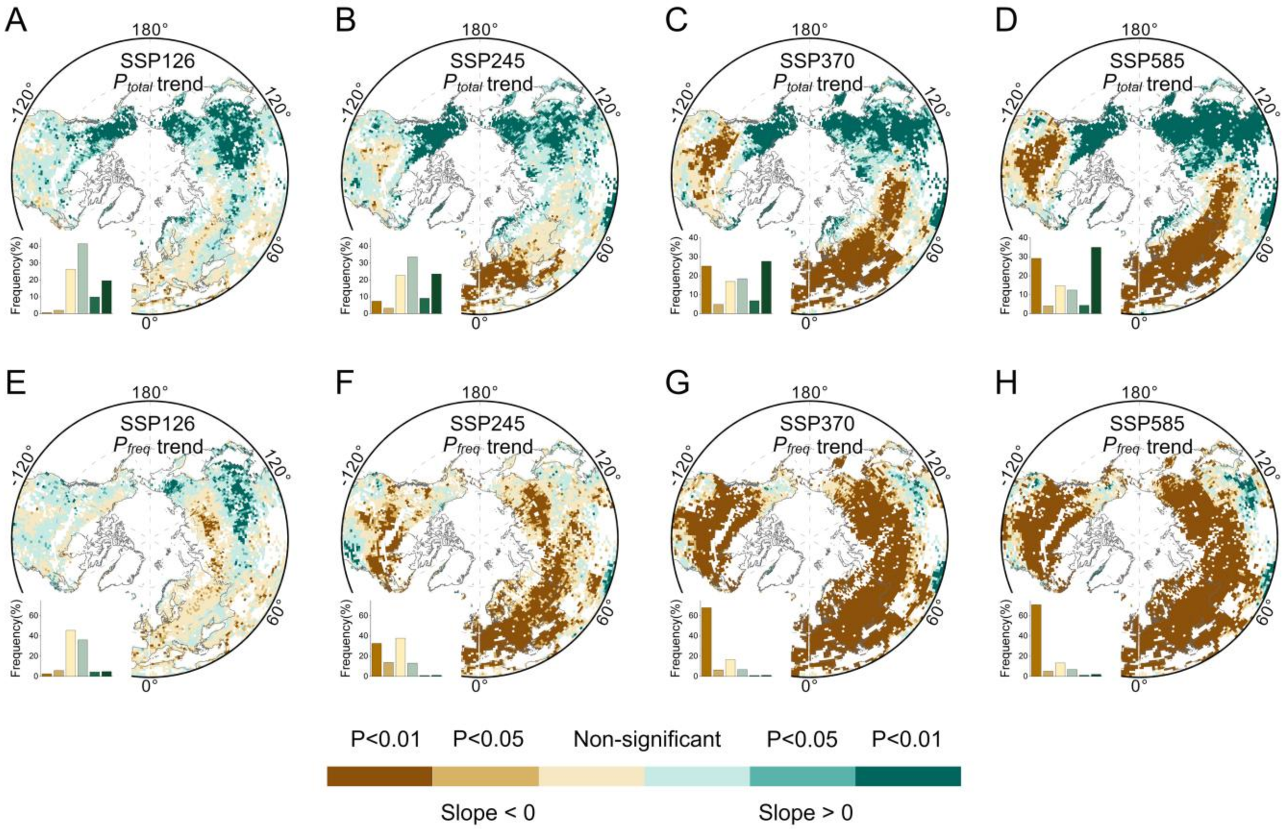

Figure S3 Changes in total precipitation (P_{total}) under various shared socioeconomic pathways (SSPs) of (A) SSP126, (B) SSP245, (C) SSP370, and (D) SSP585. E-H represent the precipitation frequency (P_{freq}) for these four SSPs, respectively.

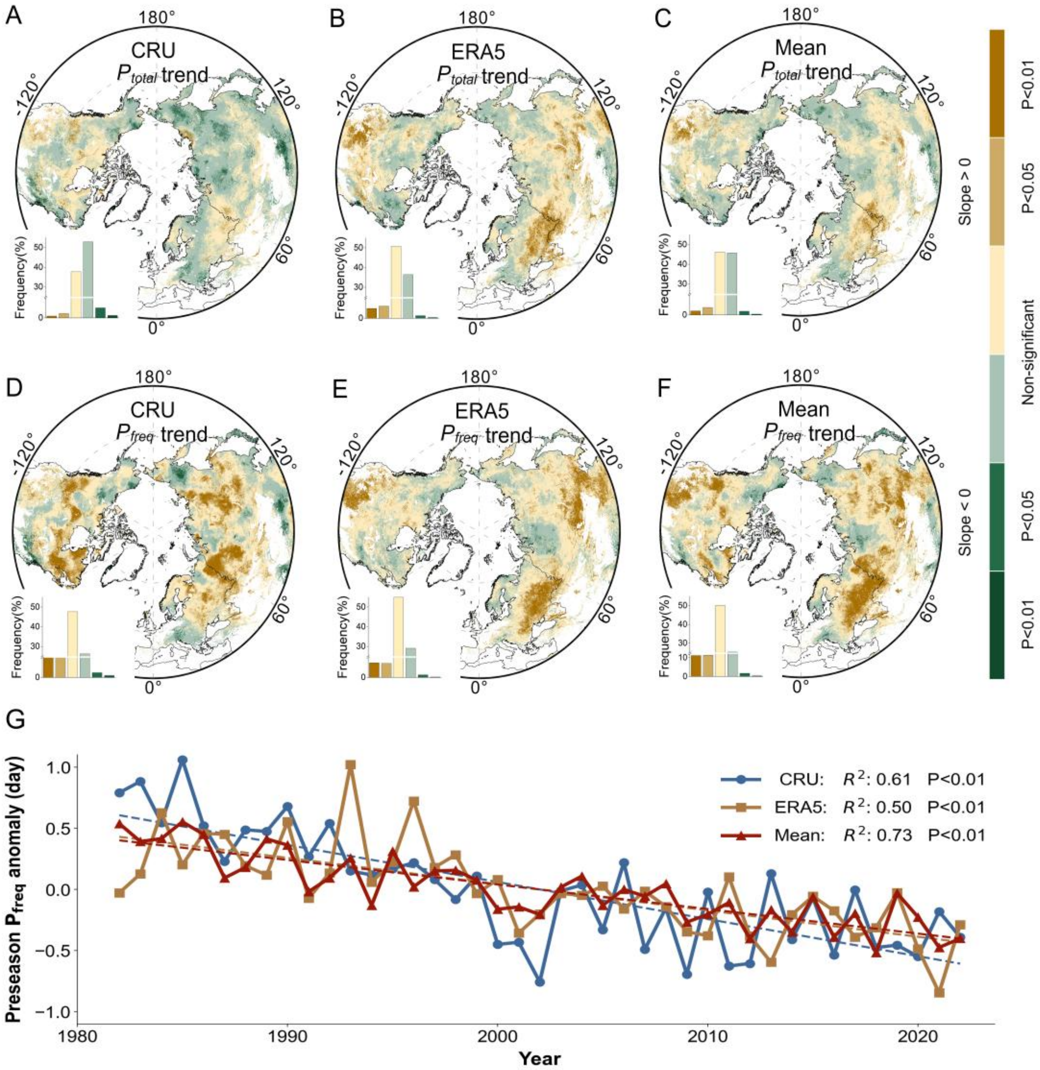

Figure S4 Changes in total precipitation (P_{total}, mm/y), precipitation frequency (P_{freq}, n/y) and its mean for the CRU (A-C) and ERA5 (D-F) observations over the Northern Hemisphere. G shows the yarly trends of P_{freq} for the two observations.

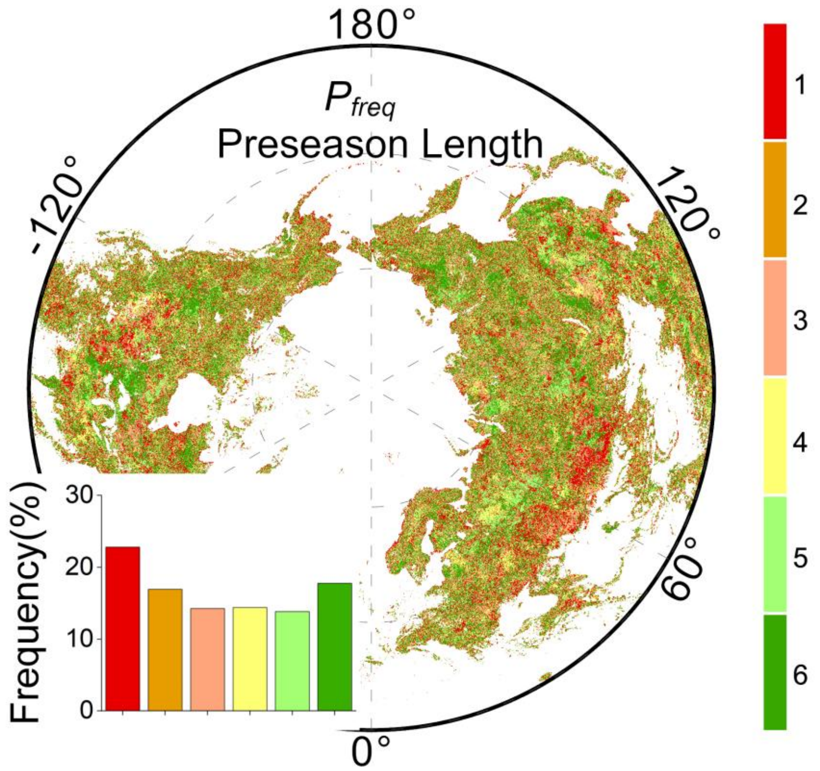

Figure S5 Distribution of the preseason length for precipitation frequency over the Northern Hemisphere.

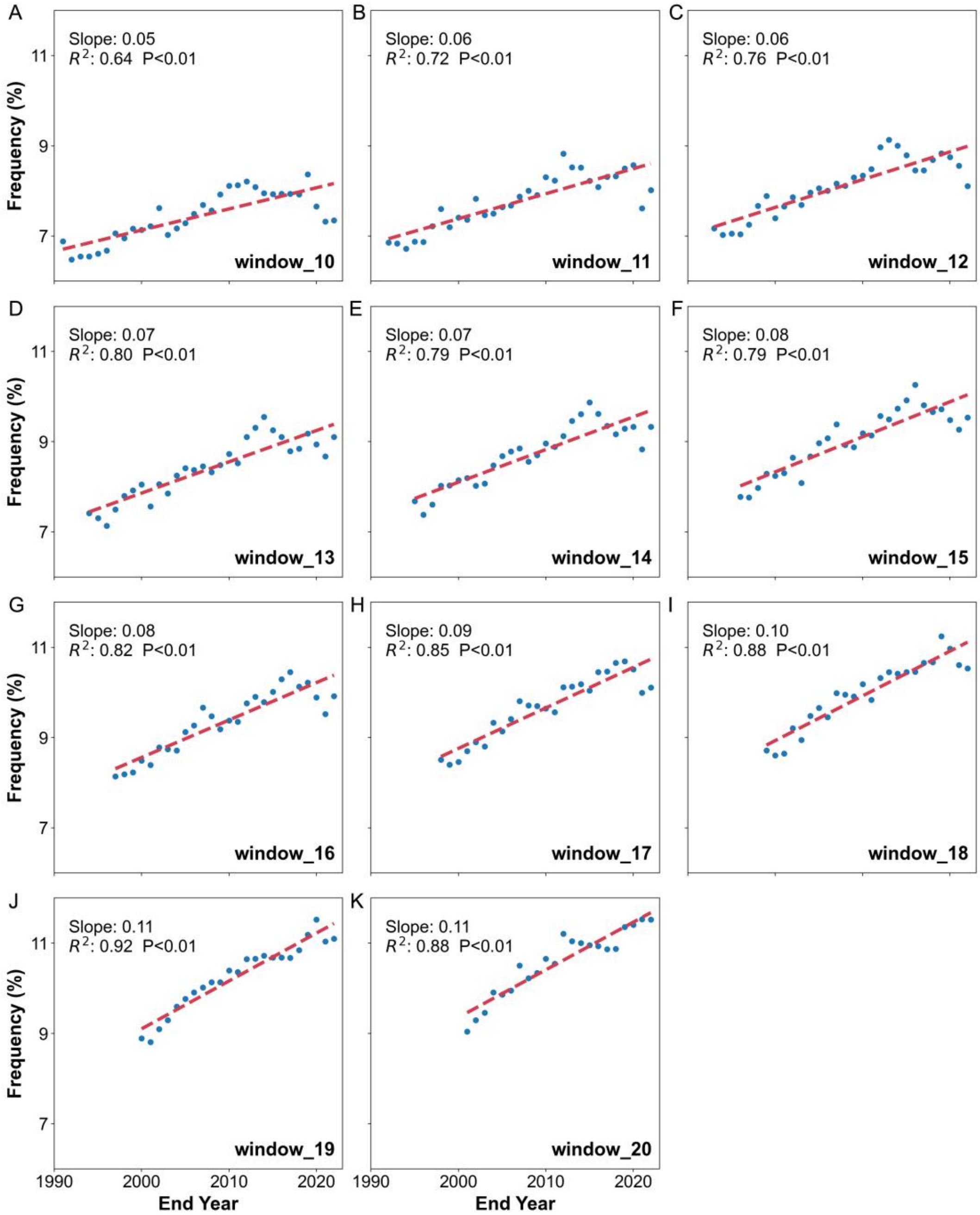

Figure S6 The determination of the optimal size of moving window approach. A-K represent the window size of 10-20 years, respectively.

Table S1 Descriptions of the data used in this study.

#	Variable name	Spatial resolution	Temporal resolution	Time range	Source
1	GIMMS NDVI3g	0.0833°	half-monthly	1982-2022	GIMMS[1]
2	Plant functional type	-	-	2001	Ref. (1)[2]
3	2m temperature	0.1°	monthly	1982-2022	ERA5[3]
4	Total precipitation	0.1°	monthly	1982-2022	ERA5[3]
5	Solar radiation	0.1°	monthly	1982-2022	ERA5[3]
6	Hourly precipitation	0.1°	hourly	1982-2022	ERA5[4]
7	Total precipitation	0.5°	monthly	1982-2022	CRU[5]
8	Precipitation frequency	0.5°	monthly	1982-2022	CRU[5]
9	Evapotranspiration	0.042°	monthly	1982-2022	TerraClimate[6]
10	Vapor pressure deficit (VPD)	0.042°	monthly	1982-2022	TerraClimate[6]
11	Root-Zone Soil Moisture	0.25°	monthly	1982-2022	GLEAM[7]
12	Root depth	0.0083°	-	-	Ref. (2)[8]
13	Drought response lag	0.0833°	-	-	Ref. (3)[9]
13	Drought recovery time	0.0833°	-	-	Ref. (3)[9]

[1]https://climatedataguide.ucar.edu/climate-data/ndvi-normalized-difference-vegetation-index-3rd-generation-nasagfsc-gimms

[2]https://www.worldwildlife.org/publications/terrestrial-ecoregions-of-the-world

[3]https://cds.climate.copernicus.eu/cdsapp - !/dataset/reanalysis-era5-land-monthly-means?tab=form

[4]https://cds.climate.copernicus.eu/cdsapp#!/dataset/reanalysis-era5-land?tab=overview

[5]https://crudata.uea.ac.uk/cru/data//hrg/

[6]https://climate.northwestknowledge.net/TERRACLIMATE/index_animations.php/

[7]https://www.gleam.eu/

[8]https://wci.earth2observe.eu/thredds/catalog/usc/root-depth/catalog.html

[9]https://doi.org/10.1038/s41558-022-01584-2

Table S2 Descriptions of the flux sites used in this study.

#	SITE	IGBP	LAT	LON	number	Start year	End year
1	AT-Neu	GRA	47.1167	11.3175	11	2003	2012
2	BE-Bra	MF	51.3092	4.5206	15	2000	2013
3	BE-Vie	MF	50.3051	5.9981	18	1998	2014
4	CA-Gro	MF	48.2167	-82.1556	10	2005	2013
5	CA-Man	ENF	55.8796	-98.4808	14	1995	2007
6	CA-Oas	DBF	53.6289	-106.198	15	1997	2010
7	CA-Obs	ENF	53.9872	-105.118	11	2001	2010
8	CA-TP1	ENF	42.6609	-80.5595	11	2005	2014
9	CA-TP3	ENF	42.7068	-80.3483	12	2004	2014
10	CA-TP4	ENF	42.7102	-80.3574	12	2004	2014
11	CH-Cha	GRA	47.2102	8.4104	10	2006	2014
12	CH-Dav	ENF	46.8153	9.8559	18	1998	2014
13	CH-Fru	GRA	47.1158	8.5378	9	2007	2014
14	CH-Lae	MF	47.4781	8.365	10	2006	2014
15	CZ-wet	WET	49.0247	14.7704	9	2007	2014
16	DE-Gri	GRA	50.95	13.5126	11	2005	2014
17	DE-Hai	DBF	51.0792	10.453	13	2001	2012
18	DE-Lnf	DBF	51.3282	10.3678	8	2003	2009
19	DE-Tha	ENF	50.9624	13.5652	18	1998	2014
20	DK-Sor	DBF	55.4859	11.6446	18	1998	2014
21	DK-ZaH	GRA	74.4732	-20.5503	12	2001	2011
22	FI-Hyy	ENF	61.8474	24.2948	18	1998	2014
23	FI-Sod	ENF	67.3619	26.6378	14	2002	2014
24	FR-Fon	DBF	48.4764	2.7801	10	2006	2014
25	FR-LBr	ENF	44.7171	-0.7693	12	1998	2008
26	FR-Pue	EBF	43.7414	3.5958	15	2001	2014
27	IT-Col	DBF	41.8494	13.5881	18	1998	2014
28	IT-Cpz	EBF	41.7052	12.3761	8	2002	2008

29	IT-Lav	ENF	45.9562	11.2813	12	2004	2014
30	IT-MBo	GRA	46.0147	11.0458	11	2004	2013
31	IT-Ren	ENF	46.5869	11.4337	13	2000	2011
32	IT-Ro1	DBF	42.4081	11.93	8	2002	2008
33	IT-Ro2	DBF	42.3903	11.9209	10	2003	2011
34	IT-SRo	ENF	43.7279	10.2844	13	2001	2012
35	NL-Loo	ENF	52.1666	5.7436	17	1998	2013
36	RU-Cok	OSH	70.8291	147.4943	11	2004	2013
37	RU-Fyo	ENF	56.4615	32.9221	16	2000	2014
38	RU-Sam	GRA	72.3738	126.4958	11	2003	2012
39	US-GLE	ENF	41.3667	-106.24	10	2006	2014
40	US-Ha1	DBF	42.5378	-72.1715	21	1993	2012
41	US-Los	WET	46.0827	-89.9792	9	2002	2009
42	US-MMS	DBF	39.3232	-86.4131	16	2000	2014
43	US-Me2	ENF	44.4523	-121.557	13	2003	2014
44	US-NR1	ENF	40.0329	-105.546	16	2000	2014
45	US-Oho	DBF	41.5545	-83.8438	10	2005	2013
46	US-PFa	MF	45.9459	-90.2723	18	1998	2014
47	US-Syv	MF	46.242	-89.3477	10	2002	2010
48	US-UMB	DBF	45.5598	-84.7138	15	2001	2014
49	US-Var	GRA	38.4133	-120.951	14	2002	2014
50	US-WCr	DBF	45.8059	-90.0799	12	2000	2010
51	US-Whs	OSH	31.7438	-110.052	8	2008	2014
52	US-Wkg	GRA	31.7365	-109.942	8	2008	2014

Table S3 Description of Trendy models

#	Model name	Spatial resolution	Temporal	Time range	Source
1	CABLE-POP	1°×1°	monthly	1983-2021	Ref. (4)[1]
2	CLASSIC	1°×1°	monthly	1983-2021	Ref. (5)[1]
3	CLM5.0	1.25°×0.9375°	monthly	1983-2021	Ref. (6)[1]
4	DLEM	0.5°×0.5°	monthly	1983-2021	Ref. (7)[1]
5	IBIS	1°×1°	monthly	1983-2021	Ref. (8)[1]
6	ISAM	0.5°×0.5°	monthly	1983-2021	Ref. (9)[1]
7	JSBACH	1.875°×1.875°	monthly	1983-2021	Ref. (10)[1]
8	JULES	1.875°×1.25°	monthly	1983-2021	Ref. (10) [1]
9	LPJ-GUESS	0.5°×0.5°	monthly	1983-2021	Ref. (12)[1]
10	LPX-Bern	0.5°×0.5°	monthly	1983-2021	Ref. (13)[1]
11	OCN	1°×1°	monthly	1983-2021	Ref. (14)[1]
12	ORCHIDEE	0.5°×0.5°	monthly	1983-2021	Ref. (15)[1]
13	SDGVM	1°x1°	monthly	1983-2021	Ref. (16)[1]
14	VISIT-NIES	0.5°×0.5°	monthly	1983-2021	Ref. (17)[1]
15	VISIT	0.5°×0.5°	monthly	1983-2021	Ref. (18)[1]
16	YIBs	1°×1°	monthly	1983-2021	Ref. (19)[1]

1 https://blogs.exeter.ac.uk/trendy/

Table S4 Description of Cmip6 models

#	Model name	Spatial resolution	Temporal	Time range	Source
1	ACCESS-ESM1-5	1.875°×1.25°	monthly	2016-2100	Ref. (20)[1]
2	BCC-CSM2-MR	1.125°×1.125°	monthly	2016-2100	Ref. (21)[1]
4	CESM2-WACCM	1.25°×0.9375°	monthly	2016-2100	Ref. (22)[1]
5	CMCC-CM2-SR5	1.25°×0.9375°	monthly	2016-2100	Ref. (23)[1]
6	CMCC-ESM2	1.25°×0.9375°	monthly	2016-2100	Ref. (24)[1]
7	EC-Earth3-Veg	0.7031°×0.7031°	monthly	2016-2100	Ref. (25)[1]
8	EC-Earth3-Veg-LR	1.125°×1.125°	monthly	2016-2100	Ref. (26)[1]
9	INM-CM4-8	2.0°×1.5°	monthly	2016-2100	Ref. (27)[1]
10	INM-CM5-0	2.0°×1.5°	monthly	2016-2100	Ref. (28)[1]
11	IPSL-CM6A-LR	2.5°×1.25°	monthly	2016-2100	Ref. (29)[1]
12	MPIESM1-2-HR	0.9375°×0.9375°	monthly	2016-2100	Ref. (30)[1]
13	MPIESM1-2-LR	1.875°×1.875°	monthly	2016-2100	Ref. (31)[1]
14	NorESM2-MM	1.25°×0.9375°	3-hourly	2016-2100	Ref. (32)[1]
15	TaiESM1	1.25°×0.9375°	monthly	2016-2100	Ref. (33)[1]

1 https://esgf-node.llnl.gov/projects/cmip6/

Supplementary References

1. Olson, D. M. *et al.* Terrestrial Ecoregions of the World: A New Map of Life on Earth: A new global map of terrestrial ecoregions provides an innovative tool for conserving biodiversity. *BioScience* **51**, 933–938 (2001).
2. Fan, Y., Miguez-Macho, G., Jobbágy, E. G., Jackson, R. B. & Otero-Casal, C. Hydrologic regulation of plant rooting depth. *Proc. Natl. Acad. Sci.* **114**, 10572–10577 (2017).
3. Li, Y. *et al.* Widespread spring phenology effects on drought recovery of Northern Hemisphere ecosystems. *Nat. Clim. Change* **13**, 182–188 (2023).
4. Haverd, V. *et al.* A new version of the CABLE land surface model (Subversion revision r4601) incorporating land use and land cover change, woody vegetation demography, and a novel optimisation-based approach to plant coordination of photosynthesis. *Geosci. Model Dev.* **11**, 2995–3026 (2018).
5. Melton, J. R. *et al.* CLASSIC v1.0: the open-source community successor to the Canadian Land Surface Scheme (CLASS) and the Canadian Terrestrial Ecosystem Model (CTEM) – Part 1: Model framework and site-level performance. *Geosci. Model Dev.* **13**, 2825–2850 (2020).
6. Lawrence, D. M. *et al.* The Community Land Model Version 5: Description of New Features, Benchmarking, and Impact of Forcing Uncertainty. *J. Adv. Model. Earth Syst.* **11**, 4245–4287 (2019).
7. Tian, H. *et al.* North American terrestrial CO2 uptake largely offset by CH4 and N2O emissions: toward a full accounting of the greenhouse gas budget. *Clim. Change* **129**, 413–426 (2015).
8. Foley, J. A. *et al.* An integrated biosphere model of land surface processes, terrestrial carbon balance, and vegetation dynamics. *Glob. Biogeochem. Cycles* **10**, 603–628 (1996).
9. Meiyappan, P., Jain, A. K. & House, J. I. Increased influence of nitrogen limitation on CO2 emissions from future land use and land use change. *Glob. Biogeochem. Cycles* **29**, 1524–1548 (2015).
10. Reick, C. H. *et al.* JSBACH 3 - The land component of the MPI Earth System Model: documentation of version 3.2. (2021) doi:10.17617/2.3279802.
11. Clark, D. B. *et al.* The Joint UK Land Environment Simulator (JULES), model description – Part 2: Carbon fluxes and vegetation dynamics. *Geosci. Model Dev.* **4**,

701–722 (2011).

12. Smith, B. *et al.* Implications of incorporating N cycling and N limitations on primary production in an individual-based dynamic vegetation model. *Biogeosciences* **11**, 2027–2054 (2014).
13. Lienert, S. & Joos, F. A Bayesian ensemble data assimilation to constrain model parameters and land-use carbon emissions. *Biogeosciences* **15**, 2909–2930 (2018).
14. Zaehle, S. & Friend, A. D. Carbon and nitrogen cycle dynamics in the O-CN land surface model: 1. Model description, site-scale evaluation, and sensitivity to parameter estimates. *Glob. Biogeochem. Cycles* **24**, (2010).
15. Krinner, G. *et al.* A dynamic global vegetation model for studies of the coupled atmosphere-biosphere system. *Glob. Biogeochem. Cycles* **19**, (2005).
16. Walker, A. P. *et al.* The impact of alternative trait-scaling hypotheses for the maximum photosynthetic carboxylation rate (Vcmax) on global gross primary production. *New Phytol.* **215**, 1370–1386 (2017).
17. Yosuke Niwa. Long-term global CO2 fluxes estimated by NICAM-based Inverse Simulation for Monitoring CO2 (NISMON-CO2). *National Institute for Environmental Studies, Japan* http://www.nies.go.jp/doi/10.17595/20201127.001-e.html.
18. Kato, E., Kinoshita, T., Ito, A., Kawamiya, M. & Yamagata, Y. Evaluation of spatially explicit emission scenario of land-use change and biomass burning using a process-based biogeochemical model. *J. Land Use Sci.* **8**, 104–122 (2013).
19. Yue, X. & Unger, N. The Yale Interactive terrestrial Biosphere model version 1.0: description, evaluation and implementation into NASA GISS ModelE2. *Geosci. Model Dev.* **8**, 2399–2417 (2015).
20. Ziehn, T. *et al.* CSIRO ACCESS-ESM1.5 model output prepared for CMIP6 ScenarioMIP. (2019) doi:10.22033/ESGF/CMIP6.2291.
21. Xin, X. *et al.* BCC BCC-CSM2MR model output prepared for CMIP6 ScenarioMIP. (2019) doi:10.22033/ESGF/CMIP6.1732.
22. Danabasoglu, G. NCAR CESM2-WACCM model output prepared for CMIP6 ScenarioMIP. (2019) doi:10.22033/ESGF/CMIP6.10026.
23. Lovato, T. & Peano, D. CMCC CMCC-CM2-SR5 model output prepared for CMIP6 ScenarioMIP. (2020) doi:10.22033/ESGF/CMIP6.1365.
24. Lovato, T., Peano, D. & Butenschön, M. CMCC CMCC-ESM2 model output prepared for CMIP6 ScenarioMIP. (2021) doi:10.22033/ESGF/CMIP6.13168.
25. Consortium (EC-Earth), E.-E. EC-Earth-Consortium EC-Earth3-Veg model output

prepared for CMIP6 ScenarioMIP. (2019) doi:10.22033/ESGF/CMIP6.727.

26. Döscher, R. *et al.* The EC-Earth3 Earth system model for the Coupled Model Intercomparison Project 6. *Geosci. Model Dev.* **15**, 2973–3020 (2022).
27. Volodin, E. *et al.* INM INM-CM4-8 model output prepared for CMIP6 CMIP piControl. (2019) doi:10.22033/ESGF/CMIP6.5080.
28. Volodin, E. *et al.* INM INM-CM5-0 model output prepared for CMIP6 CMIP piControl. (2019) doi:10.22033/ESGF/CMIP6.5081.
29. Boucher, O. *et al.* IPSL IPSL-CM6A-LR model output prepared for CMIP6 ScenarioMIP. (2019) doi:10.22033/ESGF/CMIP6.1532.
30. Müller, W. A. *et al.* A Higher-resolution Version of the Max Planck Institute Earth System Model (MPI-ESM1.2-HR). *J. Adv. Model. Earth Syst.* **10**, 1383–1413 (2018).
31. Giorgetta, M. A. *et al.* Climate and carbon cycle changes from 1850 to 2100 in MPI-ESM simulations for the Coupled Model Intercomparison Project phase 5. *J. Adv. Model. Earth Syst.* **5**, 572–597 (2013).
32. Bentsen, M. *et al.* NCC NorESM2-MM model output prepared for CMIP6 ScenarioMIP. (2019) doi:10.22033/ESGF/CMIP6.608.
33. Lee, W.-L. & Liang, H.-C. AS-RCEC TaiESM1.0 model output prepared for CMIP6 ScenarioMIP. (2020) doi:10.22033/ESGF/CMIP6.9688.